

Low Complexity Neural Network Structures for Self-Interference Cancellation in Full-Duplex Radio

Mohamed Elsayed, *Student Member, IEEE*, Ahmad A. Aziz El-Banna, *Member, IEEE*, Octavia A. Dobre, *Fellow, IEEE*, Wanyi Shiu, and Peiwei Wang

Abstract

Self-interference (SI) is considered as a main challenge in full-duplex (FD) systems. Therefore, efficient SI cancelers are required for the influential deployment of FD systems in beyond fifth-generation wireless networks. Existing methods for SI cancellation have mostly considered the polynomial representation of the SI signal at the receiver. These methods are shown to operate well in practice while requiring high computational complexity. Alternatively, neural networks (NNs) are envisioned as promising candidates for modeling the SI signal with reduced computational complexity. Consequently, in this paper, two novel low complexity NN structures, referred to as the ladder-wise grid structure (LWGS) and moving-window grid structure (MWGS), are proposed. The core idea of these two structures is to mimic the non-linearity and memory effect introduced to the SI signal in order to achieve proper SI cancellation while exhibiting low computational complexity. The simulation results reveal that the LWGS and MWGS NN-based cancelers attain the same cancellation performance of the polynomial-based canceler while providing 49.87% and 34.19% complexity reduction, respectively.

Index Terms

Full-duplex (FD), self interference (SI) cancellation, cascade correlation neural network (CasCor NN), complex-valued feed-forward NN (CV-FFNN), computational complexity.

This work is supported by Huawei Canada Research Centre, Huawei Technologies, Canada.

M. Elsayed, A. A. A. El-Banna, and O. A. Dobre are with the Faculty of Engineering and Applied Science, Memorial University, St. John's, NL A1B 3X5, Canada (e-mail: {memselim, aaelbanna, odobre}@mun.ca).

A. A. A. El-Banna is also on leave from the Faculty of Engineering at Shoubra, Benha University, Banha, Egypt.

W. Shiu and P. Wang are with Huawei Canada Research Centre, Huawei Technologies Canada Co., Ltd., Ottawa, ON K2K 3J1, Canada (e-mail: {wanyi.shiu, peiwei.wang}@huawei.com).

I. INTRODUCTION

The recent advancements in wireless technology impose a tremendous increase in the number of devices that are required to satisfy the ascending demand for high data rates communication. This high increase leads to an undeniable fact that some levels of saturation in the available frequency resources will be reached. Therefore, using efficient methods for sharing the spectrum resources is eagerly mandated for the next generations of wireless systems, such as beyond the fifth-generation [1]. The full-duplex (FD) technology has emerged as a promising remedy for the spectrum congestion problem by providing an efficient way for spectrum sharing. In the FD systems, the data is transmitted and received at the same time slot and in the same band of frequency [2]. Sharing the spectrum resources simultaneously has the potential of doubling the spectral efficiency of the FD systems. However, this in turn, gives rise to a substantial problem known as the self-interference (SI), which occurs when the transmitter's signal is leaked into the FD receiver. As such, canceling the SI signal at the receiver is deemed the main challenge against the practical deployment of FD systems [3], [4].

For typical FD systems, the SI signal could be 110 dB larger than the desired signal of interest at the receiver [5]. Therefore, if not efficiently eliminated, the SI signal may saturate the receiver's analog components, such as the analog-to-digital converter (ADC) and the low-noise amplifier (LNA) [2]. Existing methods for SI cancellation employ analog domain cancellation techniques, which are performed either passively using the physical separation between the transmit and receive antennas or actively by injecting a cancellation waveform into the propagation path of the received signal [3]. However, the analog cancellation techniques are not usually able to completely eliminate the SI signal at the receiver. Hence, the residual amount of the SI signal is further suppressed with the help of digital domain cancellation [6]. For that, the digital transmitted signal is subtracted from the received signal to perform the SI cancellation. The digital cancellation procedure seems to be an easy task in theory; however, it is hard to be realized in practice due to the non-linear distortion caused by the various parts of the transceiver, such as the power amplifier (PA), IQ mixer, ADC, and digital-to-analog converter (DAC) [7]. This distortion makes the SI signal entirely different from the digital transmitted signal and raises a challenge for the perfect elimination of the SI signal at the receiver. Typically, the polynomial model is used for modeling the non-linearities caused by different parts of the FD transceiver. The polynomial model works properly in practice while suffering from high computational complexity [8].

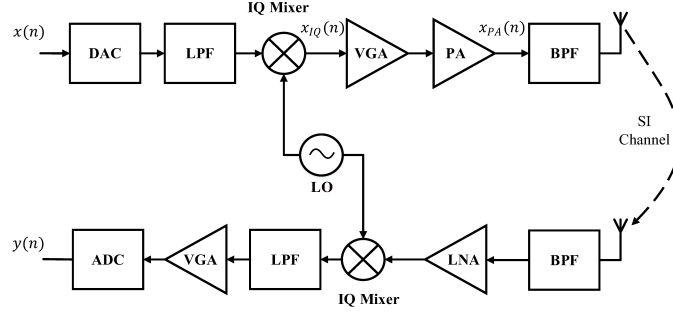


Fig. 1: Full-duplex transceiver system model.

Recently, neural networks (NNs) have received remarkable research interest from communication community experts due to their advantages in modeling the non-linearities with reduced computational complexity [8]–[11]. In [8], the authors introduce a real-valued feed-forward NN (RV-FFNN) to model the SI signal. Further, the hardware implementation of this NN-based canceler is presented in [10]. The same research group proposes the complex-valued FFNN (CV-FFNN) to perform the SI cancellation, and shows that the CV-FFNN could achieve the same cancellation as the RV-FFNN with a reduced number of floating-point operations (FLOPs) [11]. In addition, in [11], the recurrent NN (RNN) is introduced for SI cancellation due to its capability to model data sequences; it has been shown that the RNN is not a proper candidate solution for the SI cancellation problem due to its high computational complexity. To the best of our knowledge, the research works of [8] and [11] represent the few attempts that target the application of NNs for SI cancellation in FD systems, and there is a scarcity of contributions in this field.

Subsequently, in this paper, two novel NN structures, referred to as the ladder-wise grid structure (LWGS) and moving-window grid structure (MWGS), are proposed. The aim of these structures is to model the SI signal with low computational complexity. The proposed NNs exploit a grid topology in which only partial connections among the different neurons in the input and hidden layers are utilized to model the SI signal with reduced computational complexity. In addition, the proposed methods aim to learn the memory effect introduced to the SI signal in order to efficiently perform the SI cancellation. The numerical simulations substantiate the validity of the proposed LWGS and MWGS NN-based cancelers as they achieve the same cancellation performance of the polynomial canceler while providing 49.87% and 34.19% reduction in the number of FLOPs, respectively. Besides, the proposed LWGS and MWGS outperform the state-of-the-art NN-based cancelers in terms of computational complexity.

II. FULL-DUPLEX SYSTEM MODEL

The system model of the FD transceiver is depicted in Fig. 1. In this paper, the polynomial model is used to approximate the SI signal. Therefore, we follow the stipulated assumption in [7] that the IQ mixer and PA are considered the dominant sources of non-linearities in the FD transceiver. Accordingly, the non-linear effect of other transceiver components, such as the DAC, ADC, variable gain amplifier (VGA), and LNA, is neglected. Furthermore, due to the use of a shared local oscillator (LO) for both transmitter and receiver, the effect of the phase noise is also ignored [10]. As such, the digital transmitted signal $x(n)$ is firstly converted from the digital to analog form using the DAC. The analog signal is then filtered using a low pass filter (LPF) and mixed with the carrier signal at the IQ mixer. The IQ mixer adds a non-linear distortion to the input signal due to the IQ imbalance, and the digital equivalent of the IQ mixer signal can be written as [7]

$$x_{IQ}(n) = \frac{1}{2}(1 + \psi e^{j\theta}) x(n) + \frac{1}{2}(1 - \psi e^{j\theta}) x^*(n), \quad (1)$$

where ψ and θ denote the transmitter's gain and phase imbalance parameters, respectively. The mixed signal is then amplified using the PA, which further distorts the input signal by adding additional non-linearities. In this paper, we consider the parallel Hammerstein model to approximate the non-linear distortion of the PA [7]. Subsequently, the output signal of the PA can be expressed as follows [7], [8]:

$$x_{PA}(n) = \sum_{\substack{p=1, \\ p \text{ odd}}}^P \sum_{m=0}^{M_{PA}} h_{m,p} x_{IQ}(n-m)^{\frac{p+1}{2}} x_{IQ}^*(n-m)^{\frac{p-1}{2}}, \quad (2)$$

where $h_{m,p}$ represents the impulse response of the parallel Hammerstein model, while P and M_{PA} are the non-linearity order and memory length of the PA, respectively.

The amplified signal is then leaked into the receiver via the SI channel forming the SI signal. With the assumption that the FD system does not receive any signal from any remote FD nodes (i.e., no signal of interest is considered) and there is no thermal noise, only the SI signal will go through the receiver. The received SI signal is firstly filtered by the band pass filter (BPF), then amplified by the LNA, down-converted by means of the IQ mixer, and finally converted to digital form using the ADC. The SI signal at the receiver output is expressed as

$$y(n) = \sum_{\substack{p=1, \\ p \text{ odd}}}^P \sum_{q=0}^p \sum_{m=0}^{M-1} h_{m,q,p} x(n-m)^q x^*(n-m)^{p-q}, \quad (3)$$

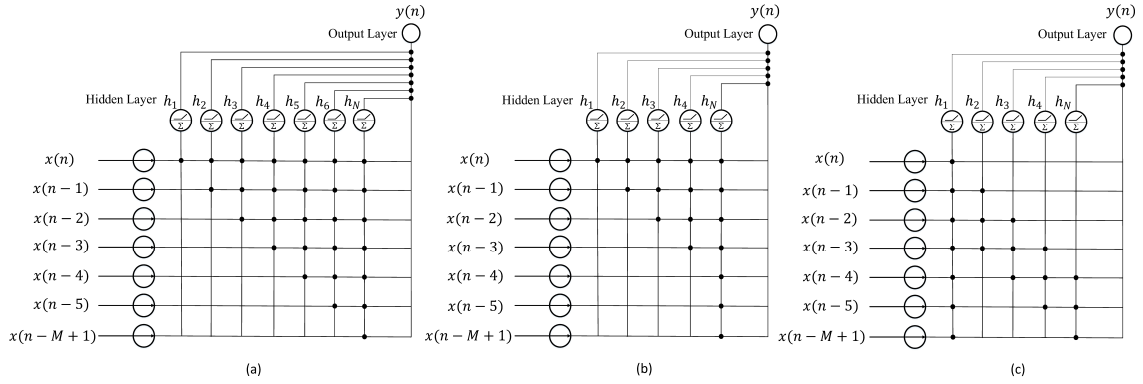


Fig. 2: Proposed NNs (a) LWGS for $N = M$ (b) LWGS for $N < M$ (c) MWGS.

where $h_{m,q,p}$ indicates the impulse response of a channel including the overall effect of the PA, IQ mixer, and SI channel, while M denotes the memory effect introduced to the input signal by the PA and SI channel.

The main aim of the digital canceler is to generate an accurate estimated version $\hat{y}(n)$ of the SI signal $y(n)$ at the receiver. Therefore, to perform the digital SI cancellation, $\hat{y}(n)$ is subtracted from $y(n)$, and the residual amount of the SI is approximated as $y_r(n) = y(n) - \hat{y}(n)$. Hence, the amount of SI cancellation can be given in dB as

$$\Psi_{dB} = 10 \log_{10} \left(\frac{\sum_n |y(n)|^2}{\sum_n |y_r(n)|^2} \right). \quad (4)$$

III. PROPOSED NN-BASED CANCELERS

Cascade forward NN is an NN architecture that utilizes additional connections from the input and every pre-layer to every post-layer [12]. The cascade forward NN has been broadly utilized to model the time series data, and it is shown to work well in a wide variety of problems [12]. A similar NN that employs a cascade structure is the cascade correlation NN (CasCor NN) [13], a promising solution to speed up the learning algorithms of the conventional NNs, such as the back-propagation. CasCor NN starts with a simple network topology that contains only input and output units, and then successively adds hidden units one by one until the desired level of network error is accomplished. The resulting network is formed in a grid topology in which each new added unit is connected to the input and other layers' units in a cascade structure fashion.

CasCor NN has a faster learning capability than the conventional NNs that apply back-propagation algorithms. Moreover, it is not mandatory in CasCor NN to determine the network structure before the training phase since the network automatically determines its optimum configuration [13]. However, the major disadvantage of CasCor NN is that it potentially overfits

to the training data in the sense that it yields a better performance on the training set while achieving worse performance on a previously unseen (i.e., new) data [14]. As a result, modified versions of CasCor NN have been introduced to avoid the overfitting of CasCor NN by applying simplified grid structures with only partial connections in the grid [15]. Based on this, for the SI cancellation, various grid structures can be investigated to model the memory effect introduced to the SI signal in order to achieve a desired cancellation performance with reduced computational complexity.

Motivated by this promising idea, two novel low complexity NN structures, named as the LWGS and MWGS, are proposed. The proposed NNs employ a grid topology with partial connections among the different neurons in the input and hidden layers. The main difference between the LWGS and MWGS lies in the way utilized by each structure to pass the buffered samples of the input signal to the different neurons in the grid in order to efficiently simulate the SI signal's memory effect. The key ideas and network structures of the proposed methods are presented in detail in the following subsections.

A. Ladder-Wise Grid Structure (LWGS)

To imitate the memory effect introduced to the SI signal, the LWGS is proposed as shown in Figs. 2(a) and (b). The LWGS employs a grid structure similar to that used in the CasCor NN. However, the LWGS uses the standard back-propagation technique to minimize the network's error and cannot determine its own structure as the CasCor NN. Accordingly, in the LWGS, the network structure is selected empirically before training to achieve the target network performance.

The basic idea behind the LWGS is to feed the buffered data to the network neurons in a stair-case manner as depicted in Figs. 2(a), (b). Here, we denote the number of hidden units by N . As such, in Fig. 2(a), we consider the case when the number of hidden units is equal to the number of input units (e.g., $N = M = 7$), where M is the memory length as stated before. Starting with the stair base, the instantaneous sample $x(n)$ is passed to all the neurons, and every predecessor sample (i.e., $x(n-1)$, $x(n-2)$, ... etc.) is passed to a fewer number of neurons gradually. The oldest sample, $x(n-M+1)$, which is the least one related to the current sample $x(n)$, is allowed to be passed to only one neuron side by side with its followers. In this manner, each neuron receives the instantaneous sample plus part of the buffered samples to learn the temporal behavior of the SI signal, and the outputs of all neurons are then combined

to figure out the detected pattern. Following this approach, the LWGS could model the SI signal with only partial connections in the grid, and therefore it can result in a significant reduction in the computational complexity.

Furthermore, the LWGS can learn the memory effect introduced to the SI signal with fewer connections between the input and hidden layers' neurons. Reducing the number of connections can be done by considering a shorter length of the ladder base (i.e., reducing the number of neurons to be less than the memory length ($N < M$)) as shown in Fig. 2(b). The idea of this configuration is to enable the recent delayed samples that are more related to the instantaneous sample $x(n)$ to be learned using many neurons; however, the other samples that are less related to $x(n)$ are learned by only one neuron (e.g., $x(n - 4)$, $x(n - 5)$, $x(n - M + 1)$) in Fig. 2(b). This will slightly degrade the performance of the LWGS while providing a significant reduction in the computational complexity compared to the case when $N = M$.

In the proposed method, the SI cancellation is performed in the digital domain in which the non-linear part of the digital SI cancellation signal is reconstructed using the LWGS canceler. However, the linear part of the cancellation signal is estimated using the conventional least square channel estimation technique where all the non-linear effects of the different transceiver's components are neglected [8]. The total cancellation achieved by the LWGS canceler is then computed by summing the linear and non-linear cancellations [8], [10].

The effect of varying the number of hidden layer's neurons on the cancellation performance of the LWGS is shown in Fig. 3(a).¹ We test the LWGS using $N = 9, 10, 11, 12$ and depict the boxplots of total cancellation achieved by various configurations using 20 seed initializations. The LWGS shows flexible settings that suit different applications. For example, moving from LWGS with nine neurons (i.e., LWGS (9)) to twelve neurons (i.e., LWGS (12)) augments the SI cancellation from 44.50 to 44.75 dB; however, the increased number of neurons would result in an increased computational complexity.

B. Moving-Window Grid Structure (MWGS)

An alternative approach that can accommodate the memory effect of the SI signal is the moving window technique, generally recognized as an effective method for time series prediction [16]. As such, we consider the moving window with a grid topology to form the MWGS. Similar to the LWGS, the MWGS applies the standard back-propagation technique to minimize the

¹The results in Fig. 3 are obtained using the simulation parameters in Section V.

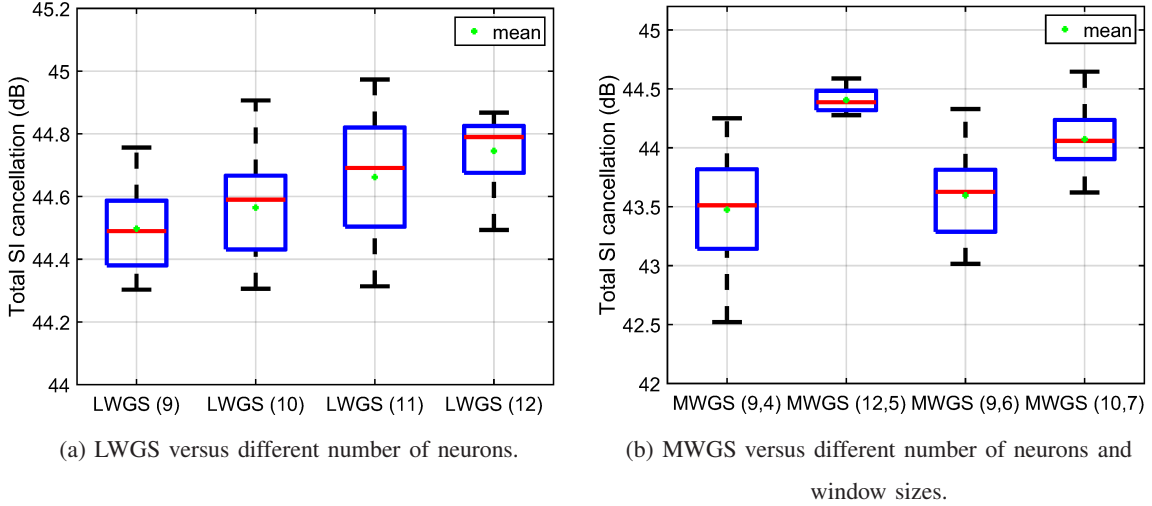


Fig. 3: SI cancellation boxplots.

network's error. Further, the MWGS takes advantage of the reduced connections in the network grid. However, in the MWGS, the considered samples of the input signals learned by different neurons are partitioned based on a fixed-length sliding window technique as depicted in Fig. 2(c). More specifically, all the input samples are passed to the first neuron. The main purpose of this neuron is to learn the dependencies between all the delayed samples of the input signal. Moreover, the other employed neurons are allowed to assist in learning the memory effect by considering the windowed data only. Besides, sliding the window over different neurons allows to consider all the buffered samples caused by the non-linearities of the aforementioned FD components. For example, in Fig. 2(c), a window size $W = 3$ is employed. Therefore, the first, second, and third delayed version of $x(n)$ (i.e., $x(n-1)$, $x(n-2)$, $x(n-3)$) are considered by the second neuron, while $x(n-2)$, $x(n-3)$, and $x(n-4)$ samples are recognized by the third neuron, and so forth.

The effect of varying the number of hidden layer's neurons N and the window size W on the cancellation performance of the MWGS is studied as well.¹ In this study, the network structures of the MWGS are selected empirically based on a trial and error approach. As such, we test the values of $N = 9, 10, 11, 12$ and $W = 4, 5, 6, 7$. Due to having many combinations between N and W , in Fig. 3(b), we only show the best four structures that achieve the highest SI cancellation. As seen from the figure, the MWGS using twelve neurons and window size $W = 5$ (i.e., MWGS (12,5)) attains the highest SI cancellation among the competing structures.

IV. COMPUTATIONAL COMPLEXITY

In this paper, we consider the total number of FLOPs as an indicator of the computational complexity of the NN-based cancelers. The total number of FLOPs is evaluated by calculating the total number of real-valued operations used in the NN's inference process as $\Xi = \Xi_{w,b} + \Xi_a$ where $\Xi_{w,b} = \xi_{w,b}^{(R_m)} + \xi_{w,b}^{(R_a)}$ is the sum of real-valued multiplications and additions, which account for multiplying the input/previous layer values by the weight matrix and adding the bias terms. Similarly, $\Xi_a = \xi_a^{(R_m)} + \xi_a^{(R_a)}$ represents the sum of real-valued multiplications and additions required to evaluate the activation functions in the hidden layer's neurons.

In the LWGS and MWGS NNs, the inputs, hidden layer values, and network parameters (e.g., weights and biases) are complex-valued numbers. Therefore, converting the complex-valued multiplications and additions to their real-valued equivalents is required. By employing the reduced multiplications approach [10], a complex-valued multiplication requires three real multiplications and five real additions. Moreover, since each complex-valued addition is implemented using two real additions, $\xi_{w,b}^{(R_m)}$ and $\xi_{w,b}^{(R_a)}$ can be expressed as

$$\xi_{w,b}^{(R_m)} = 3\xi_{w,b}^{(C_m)}, \quad (5)$$

$$\xi_{w,b}^{(R_a)} = 5\xi_{w,b}^{(C_m)} + 2\xi_{w,b}^{(C_a)}, \quad (6)$$

where $\xi_{w,b}^{(C_m)}$ and $\xi_{w,b}^{(C_a)}$ represent the number of complex-valued multiplications and additions, respectively, which account for handling the weights and biases operations.

In the LWGS, $\xi_{w,b}^{(C_m)}$ and $\xi_{w,b}^{(C_a)}$ can be calculated as

$$\xi_{w,b}^{(C_m)} = \xi_{w,b}^{(C_a)} = \sum_{i=1}^N i + M. \quad (7)$$

Further, in the MWGS, $\xi_{w,b}^{(C_m)}$ and $\xi_{w,b}^{(C_a)}$ can be obtained as

$$\xi_{w,b}^{(C_m)} = \xi_{w,b}^{(C_a)} = M + W(N - 1) + N. \quad (8)$$

However, $\xi_{w,b}^{(C_m)}$ and $\xi_{w,b}^{(C_a)}$ for CV-FFNN can be expressed as

$$\xi_{w,b}^{(C_m)} = \xi_{w,b}^{(C_a)} = N(M + 1). \quad (9)$$

The proposed LWGS and MWGS employ the complex RELU (CRELU) activation function, which is defined as [11]

$$\Phi(z) = \max(0, \Re(z)) + j \max(0, \Im(z)), \quad (10)$$

where $\Re(z)$ and $\Im(z)$ denote the real and imaginary parts of z , respectively. The implementation of \mathbb{C} RELU activation function (10) requires two real multiplications and two complex additions (i.e., four real additions) to evaluate the real and imaginary parts of z . Further, to evaluate the $\max(0, \Re(z))$ and $\max(0, \Im(z))$, two multiplexers and two comparators are required. Herein, if we assume that each comparator comes with no cost and each multiplexer costs one real addition [8], the implementation of \mathbb{C} RELU activation function requires two real multiplications and six real additions.² As such, the number of real-valued multiplications $\xi_a^{(R_m)}$ and additions $\xi_a^{(R_a)}$ utilized for evaluating the activation functions in the hidden layer's neurons of the LWGS and MWGS can be given by $\xi_a^{(R_m)} = 2N$ and $\xi_a^{(R_a)} = 6N$, respectively.

V. RESULTS AND DISCUSSION

In this section, we assess the performance of the LWGS and MWGS NN-based cancelers in terms of mean square error (MSE), SI cancellation, and computational complexity. In addition, a comparison between the proposed methods and the NN-based cancelers in the literature is also investigated. All the considered NNs are trained using complex-valued inputs and implemented in Python using Keras library and TensorFlow back-end. In this work, we examine the use of the measured dataset presented in [8] and [11]. Hence, we train and test the NNs using measured data from a realistic FD testbed, which applies an orthogonal frequency division multiplexing signal with 1024 sub-carriers using a quadrature phase-shift keying modulation and 10 MHz pass-band bandwidth. The dataset, containing 20,480 samples, is split into a training set that consists of 90% of samples and a testing set that includes the remaining 10%. We adopt the back-propagation technique, Adam optimization, and \mathbb{C} RELU activation function for the NNs [11]. The networks' hyperparameters, such as the batch size and learning rate, are tuned using five-fold cross-validation to select their optimal values. Based on cross-validation, we employ a learning rate of 0.0045 and a batch size of 62 to train the NNs. Besides, we consider $M = 13$ for the polynomial and NN-based cancelers [8], [11].

All the NN-based cancelers are employed to model the non-linear part of the SI signal. Furthermore, for the sake of comparison, the NNs settings are selected in such a way that

²We note that the activation functions' complexity in [11] is evaluated by counting their usage in the hidden layer's neurons, which is not exact.

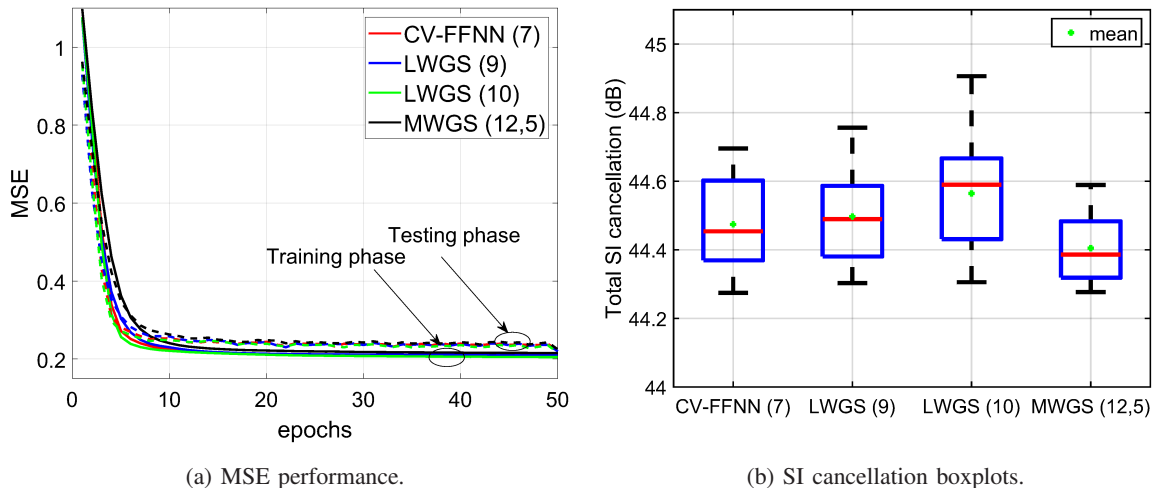


Fig. 4: Performance comparison for different network structures.

they achieve a similar cancellation performance to the polynomial canceler with $P = 5$. The polynomial canceler at $P = 5$ produces 44.45 dB cancellation and requires 1556 FLOPs and 312 network parameters to be implemented [11]. As such, to achieve the target cancellation of the polynomial canceler, the CV-FFNN requires at least a single hidden layer with seven neurons (i.e., CV-FFNN (7)) [11]. In addition, from Fig. 3, it is observed that the LWGS (9) and LWGS (10) achieve the target cancellation as they provide 44.50 and 44.56 dB, respectively. Further, the MWGS (12,5) attains 44.40 dB, which is very close to the target cancellation. Thus, in this analysis, we consider CV-FFNN (7), LWGS (9), LWGS (10), and MWGS (12,5) as promising NN-based cancelers that can be used as alternatives to the traditional polynomial canceler.

In Fig. 4(a), the MSE values of the aforementioned NNs are evaluated on the training and testing data, respectively, using 20 seed initializations. As seen from the figure, the considered NNs achieve a comparable MSE for the target cancellation performance. Fig. 4(b) depicts the boxplots of SI cancellation achieved by the considered NN-based cancelers using the above-selected settings. It is apparent from the figure that CV-FFNN (7), LWGS (9), and MWGS (12,5) attain a comparable cancellation performance to the polynomial canceler. However, LWGS (10) provides a slightly higher SI cancellation. It is worth noting that the LWGS structure slightly outperforms the cancellation of the MWGS as it passes the instantaneous sample $x(n)$ (i.e., most significant sample) to all neurons, which enables it to learn the SI signal's temporal behavior better than the MWGS.

The complexity analysis for the different NN-based cancelers is provided in Table. I, where

TABLE I: Complexity reduction for different network structures compared to the polynomial model with $P = 5$.

Network	Cancellation	Complexity		Complexity Reduction	
		# Parameters	# FLOPs	# Parameters	# FLOPs
Polynomial ($P = 5$)	44.45 dB	312	1556	-	-
CV-FFNN (7)	44.47 dB	238	1164	-23.72%	-25.19%
LWGS (9)	44.50 dB	162	780	-48.08%	-49.87%
LWGS (10)	44.56 dB	184	888	-41.03%	-42.93%
MWGS (12,5)	44.40 dB	212	1024	-32.05%	-34.19%

the polynomial canceler complexity is considered as reference, and the NNs complexity is computed in terms of the number of FLOPs and the number of network parameters used to perform the total SI cancellation (i.e., linear and non-linear cancellations). As seen from the table, the LWGS (9) reduces the number of FLOPs by more than 49% while achieving a similar cancellation to the polynomial-based canceler. Furthermore, the LWGS (10) outperforms the cancellation performance of the polynomial canceler while requiring 7% more FLOPs than the LWGS (9). Accordingly, the proposed LWGS provides a flexible trade-off between the cancellation performance and the computational complexity. In addition, the MWGS (12,5) saves 34% computations compared to the polynomial-based canceler, while the conventional CV-FFNN (7) saves only 25% of the computations. The previous results reveal the superiority of the proposed NNs compared to the polynomial and state-of-the-art NN-based cancelers.

VI. CONCLUSION

In this paper, two novel low complexity NN structures, namely the ladder-wise grid structure (LWGS) and moving-window grid structure (MWGS), are proposed to model the SI signal with low computational complexity. The former employs a stair-based structure to accommodate the memory effect of the SI signal. The latter uses a fixed-window procedure to model the temporal behavior of the SI signal. Our findings showed that the proposed LWGS and MWGS provide the same cancellation performance of the polynomial-based canceler while attaining 49.87% and 34.19% reduction in the computational complexity, respectively. In addition, the proposed LWGS and MWGS offer superior performance over the state-of-the-art NN-based cancelers by exhibiting 24.7% and 9% complexity reduction, respectively.

REFERENCES

- [1] M. Giordani, M. Polese, M. Mezzavilla, S. Rangan, and M. Zorzi, "Toward 6G networks: Use cases and technologies," *IEEE Commun. Mag.*, vol. 58, no. 3, pp. 55–61, Mar. 2020.
- [2] K. E. Kolodziej, B. T. Perry, and J. S. Herd, "In-band full-duplex technology: Techniques and systems survey," *IEEE Trans. Microw. Theory Techn.*, vol. 67, no. 7, pp. 3025–3041, Jul. 2019.
- [3] H. V. Nguyen *et al.*, "On the spectral and energy efficiencies of full-duplex cell-free massive MIMO," Sept. 2019. [Online]. Available: <https://arxiv.org/abs/1910.01294>.
- [4] F. Chen, R. Morawski, and T. Le-Ngoc, "Self-interference channel characterization for wideband 2×2 MIMO full-duplex transceivers using dual-polarized antennas," *IEEE Trans. Antennas Propag.*, vol. 66, no. 4, pp. 1967–1976, Apr. 2018.
- [5] G. Agrawal, S. Aniruddhan, and R. K. Ganti, "A compact mixer-first receiver with >24 dB self-interference cancellation for full-duplex radios," *IEEE Microw. Wireless Compon. Lett.*, vol. 26, no. 12, pp. 1005–1007, Dec. 2016.
- [6] Z. Zhang, K. Long, A. V. Vasilakos, and L. Hanzo, "Full-duplex wireless communications: Challenges, solutions, and future research directions," *Proc. IEEE*, vol. 104, no. 7, pp. 1369–1409, Jul. 2016.
- [7] D. Korpi, L. Anttila, and M. Valkama, "Nonlinear self-interference cancellation in MIMO full-duplex transceivers under crosstalk," *EURASIP J. Wireless Commun. Netw.*, vol. 2017, no. 1, pp. 1–15, Dec. 2017.
- [8] A. Balatsoukas-Stimming, "Non-linear digital self-interference cancellation for in-band full-duplex radios using neural networks," in *Proc. IEEE Int. Workshop Signal Process. Adv. Wireless Commun. (SPAWC)*, Jun. 2018, pp. 1–5.
- [9] Y. Yang, S. Zhang, F. Gao, J. Ma, and O. A. Dobre, "Graph neural network based channel tracking for massive MIMO networks," Apr. 2020. [Online]. Available: <https://arxiv.org/abs/2004.08738v1>.
- [10] Y. Kurzo, A. T. Kristensen, A. Burg, and A. Balatsoukas-Stimming, "Hardware implementation of neural self-interference cancellation," *IEEE J. Emerg. Sel. Topics Circuits Syst.*, vol. 10, no. 2, pp. 204–216, Jun. 2020.
- [11] A. T. Kristensen, A. Burg, and A. Balatsoukas-Stimming, "Advanced machine learning techniques for self-interference cancellation in full-duplex radios," in *Proc. 53rd Asilomar Conf. Signals, Syst., Comput.*, Nov. 2019, pp. 1149–1153.
- [12] B. Warsito, R. Santoso, and H. Yasin, "Cascade forward neural network for time series prediction," *J. Phys. Conf. Ser.*, vol. 1025, no. 1, pp. 1–9, May 2018.
- [13] S. E. Fahlman and C. Lebiere, "The cascade-correlation learning architecture," in *Proc. Adv. Neural Inf. Process. Syst.*, Jun. 1990, pp. 524–532.
- [14] F. J. Śmieja, "Neural network constructive algorithms: Trading generalization for learning efficiency?," *Circuits Syst., Signal Processing*, vol. 12, no. 2, pp. 331–374, Jun. 1993.
- [15] T. Y. Kwok and D. Y. Yeung, "Constructive algorithms for structure learning in feedforward neural networks for regression problems," *IEEE Trans. Neural Networks*, vol. 8, no. 3, pp. 630–645, May 1997.
- [16] D. Ruta, B. Gabrys, and C. Lemke, "A generic multilevel architecture for time series prediction," *IEEE Trans. Knowl. Data Eng.*, vol. 23, no. 3, pp. 350–359, Mar. 2011.